Available online at www.sciencedirect.com
ScienceDirect
Electrochemistry Communications 9 (2007) 2564–2570
electrochemistry communications
www.elsevier.com/locate/elecom

Functional multiwalled carbon nanotube nanocomposite with iron picket-fence porphyrin and its electrocatalytic behavior

Ying Liu, Yi-Long Yan [1], Jianping Lei *, Fan Wu, Huangxian Ju *

MOE Key Laboratory of Analytical Chemistry for Life Science, School of Chemistry and Chemical Engineering, Nanjing University, Nanjing 210093, PR China

Received 17 July 2007; received in revised form 1 August 2007; accepted 3 August 2007
Available online 10 August 2007

Abstract

A kind of nanocomposite with good dispersion in water was prepared through noncovalent adsorption of iron picket-fence porphyrin (FeTMAPP), iron-5,10,15,20-tetrakis[αααα-2-trismethylammoniomethyl-phenyl]porphyrin, on multiwalled carbon nanotubes (MWNTs). UV–visible spectroscopic and electrochemical methods were used to characterize the nanocomposite. A gold nanoparticles/nanocomposite self-assembled monolayer was formed on gold electrode and showed highly synergetic behavior towards the electrocatalytic reduction of O_2 with a decrease of overpotential of 200 mV. FeTMAPP acted as the catalytic active center, and MWNTs increased the amount of FeTMAPP adsorbed and accelerated the electron transfer between FeTMAPP and electrode. The resulting biosensor exhibited good response to oxygen with a linear range from 0.52 to 180 μM and a detection limit of 0.38 μM, without the interference of ascorbic acid and uric acid, which showed an application potential of the proposed nanocomposite and monolayer in detection of dissolved oxygen and oxidase substrates.

Keywords: Iron porphyrin; Multiwalled carbon nanotubes; Gold nanoparticles; Nanocomposites modified electrode; Amperometric sensor; Dissolved oxygen

1. Introduction

The measurement of dissolved oxygen is very important in various areas of chemical, physical and environmental monitoring [1]. Different detection systems such as fluorescence [1], chemiluminescence [2], and amperometric methods [3] have been developed for this purpose. The reduction of dissolved oxygen on electrode surfaces involves an electrochemical energy transfer process, which provides a model for study of fuel cells [4] and metal–oxygen cells [5], and a method for detection of oxidase substrates such as glucose [6,7]. Especially, the enzymatic fuel cell has earned much attention due to its high efficiency and selectivity. This work used one porphyrin derivative to assemble a nanocomposite and further a monolayer for the study of electron transfer process of dissolved oxygen.

Porphyrins are a class of naturally occurring compounds that represent many important enzymes including hemes, chlorophylls and horseradish peroxidase. The macrocyclic structure of porphyrin can conjugate many metal elements, such as Co, Fe, Ni, and Mn, to form stable complexes, which can generally be used as homogeneous catalysts in a variety of oxidation and reduction reactions and play important roles in biological transfer system, especially in the reduction of dissolved oxygen [8–11]. Among these complexes, iron porphyrins can be well used as electron media based on the reversible redox of Fe^{III}/Fe^{II}, and exhibit good electrocatalysis to many small molecules related to life process, including NO [12], neurotransmitters [13], hydrogen peroxide [14], nitrite [15], and oxygen [16,17]. However, the electrocatalysis of iron porphyrins to the

* Corresponding authors. Tel./fax: +86 25 83593593.
E-mail address: hxju@nju.edu.cn (H. Ju).
[1] Present address: Department of Chemistry and Biochemistry, University of California, San Diego, La Jolla, CA 92093-0358, USA.

1388-2481/$ - see front matter © 2007 Elsevier B.V. All rights reserved.
doi:10.1016/j.elecom.2007.08.003

reduction of dissolved oxygen is usually reported in acid solution, which limits their application in biological system.

Recently, the interactions of porphyrin and carbon nanotubes have attracted wide attention [18]. These interactions include covalent [19], electrostatic [20], and π–π noncovalent interactions [21]. The electrostatic conjugation of porphyrin on multiwalled carbon nanotubes (MWNTs) produces a well dispersion of MWNTs in water [18]. These porphyrin conjugated carbon nanotubes have been extensively used photoelectric materials. This work synthesized a kind of picket-fence porphyrin (FeTMAPP), which has four pickets around the porphyrin ring and has been considered as one of the best candidates to mimic the active sites of different enzymes [22], prepared a novel nanocomposite of picket-fence porphyrin conjugated MWNTs through π–π noncovalent interaction for its assembly on electrode surface in aid of gold nanoparticles (GNP), and proposed an application of the nanocomposite in electrocatalysis in neutral media. The resulting amperometric oxygen biosensor exhibited good stability and repeatability.

2. Experiment

2.1. Chemicals and instruments

Cysteamine ($NH_2CH_2CH_2SH$) was purchased from Sigma. MWNTs (>95%, 40–60 nm diameter) were purchased from Shenzhen Nanotech Port Ltd. Co (Shenzhen, China). All other chemicals were of analytical grade and were used as received. Aqueous solutions were prepared with doubly distilled water. 0.2 M phosphate buffer solution (PBS) was always employed as supporting electrolyte. The pH value of PBS was 7.0 except those indicated. GNP with particle size of about 20 nm was prepared according to the literature [23] and stored in brown glass bottles at 4 °C, which could keep stable for about 1 month.

Ultraviolet–visible (UV–vis) absorption spectra were recorded with a Lambda 35 UV/VIS spectrometer (Perkin-Elmer instruments, USA), the detection solution or suspension was prepared through sonication in water for 1 min. Cyclic voltammetric experiments were performed on a BAS electrochemical workstation (Epsilon, USA), and amperometric experiments were preformed on a CHI 660B electrochemical workstation (CH Instruments Inc., USA). All experiments were carried out using a conventional three-electrode system with a modified gold electrode as working, a platinum foil as auxiliary, and a saturated calomel electrode as reference electrodes.

2.2. Preparation of FeTMAPP

Iron-5,10,15,20-tetrakis[αααα-2-trismethylammoniomethyl-phenyl]porphyrin (FeTMAPP) was prepared according to Scheme 1:

αααα-TAPP (260 mg, 0.39 mmol), prepared firstly following the literature [22], was dissolved in dry CH_2Cl_2 (100 mL). Chloroacetyl chloride (0.4 mL, 5.0 mmol) was added to this solution followed by *N,N*-diethylaniline (0.5 mL, 3.2 mmol), and then the mixture was stirred at room temperature (RT) for 3 h. The reaction mixture was washed with a dilute $NaHCO_3$ solution and dried over $MgSO_4$. After concentration, the residue was purified by chromatography on silica gel with EtOAc/CH_2Cl_2 (*v*/*v*: 20/80) and then CH_3OH/CH_2Cl_2 (*v*/*v*: 5/95) to give αααα-TCPP solid (300 mg, 79%). ^{1}H NMR (500 MHz, $CDCl_3$): δ 8.76 (s, 8H), 8.66 (d, $J = 3.0$ Hz, 4H), 8.04 (d, $J = 6.5$ Hz, 4H), 7.94 (s, 4H), 7.85 (t, $J = 8.0$ Hz, 4H), 7.56 (t, $J = 7.5$ Hz, 4H), 3.35 (s, 8H), 2.64 (s, 2H); ^{13}C NMR ($CDCl_3$): 163.71, 138.04, 134.71, 131.62, 130.44, 124.12, 120.70, 114.54, 42.71; MS (ESI): $m/e = 979.3$ $[M+H]^+$ for $C_{52}H_{39}Cl_4N_8O_4$. HRMS (ESI) for $C_{52}H_{39}Cl_4N_8O_4$ $[M+H]^+$: calcd. 979.1848, found 979.1860.

αααα-TCPP (120 mg, 0.12 mmol) was stirred in a trimethylamine solution in ethyl alcohol (33%, 10 mL) overnight at RT under N_2 atmosphere. The mixture was concentrated under vacuum. The residue was recrystallized from CH_3OH/acetone solvent to give compound **1H$_2$** as a solid (112 mg, 75%). ^{1}H NMR (500 MHz, DMSO-d_6): δ 10.23 (s, 4H), 8.64 (s, 8H), 8.02 (d, $J = 8.0$ Hz, 4H), 7.97 (t, $J = 7.5$ Hz, 4H), 7.87 (d, $J = 7.5$ Hz, 4H), 7.65 (t, $J = 7.5$ Hz, 4H), 3.85 (s, 8H), 2.69 (s, 36H, NMe_3), 2.86 (s, 2H); MS (ESI): $m/e = 1180.0$ $[M-Cl]^+$ for $C_{64}H_{74}Cl_3N_{12}O_4$; HRMS (ESI) for $C_{64}H_{74}Cl_3N_{12}O_4$ $[M-Cl]^+$: calcd. 1179.5022, found 1179.5013.

The preparation of αααα-TCPP(Fe) was carried out under a N_2 atmosphere. To a solution of αααα-TCPP (200 mg, 0.2 mmol) in dry THF/benzene (20 mL, *v*/*v*: 1:1) was added $FeBr_2$ (200 mg, 0.9 mmol) followed by 2,6-lutidine (0.2 mL). The mixture was gently refluxed for 2 h. After concentration, the residue was dissolved in CH_2Cl_2 and washed with water, diluted HCl, and saturated NaCl solution. CH_2Cl_2 extract was dried over anhydrous Na_2SO_4 and then concentrated. The crude product was purified by column chromatography with eluent THF/CH_2Cl_2 (*v*/*v*: 10/90) on silica gel to give product αααα-TCPP(Fe) (182 mg, 83%) as a solid.

The preparation of FeTMAPP was also carried out under a N_2 atmosphere. αααα-TCPP(Fe) (150 mg, 0.14 mmol) was stirred in a trimethylamine solution in ethyl alcohol (33%, 15 mL) overnight at RT. Excess trimethylamine and solvent were evaporated off under vacuum. The residue was recrystallized from CH_3OH/acetone/CH_2Cl_2 to give FeTMAPP (160 mg, 88%) as a solid. MS (ESI): $m/e = 1268$ $C_{64}H_{72}Cl_4FeN_{12}O_4$ $[M-Cl]^+$; HRMS (ESI) for $C_{64}H_{72}Cl_4FeN_{12}O_4$ $[M-Cl]^+$: calcd. 1268.3903, found 1268.3926.

2.3. Preparation of MWNTs-FeTMAPP nanocomposite

1.5 mg MWNTs was added into 1 mL 1.36 mg mL^{-1} FeTMAPP solution. After the mixture was sonicated for 1 min at RT, the resulting suspension was filtered with a Millipore porous filter (0.45 μm, Millipore). The sediment

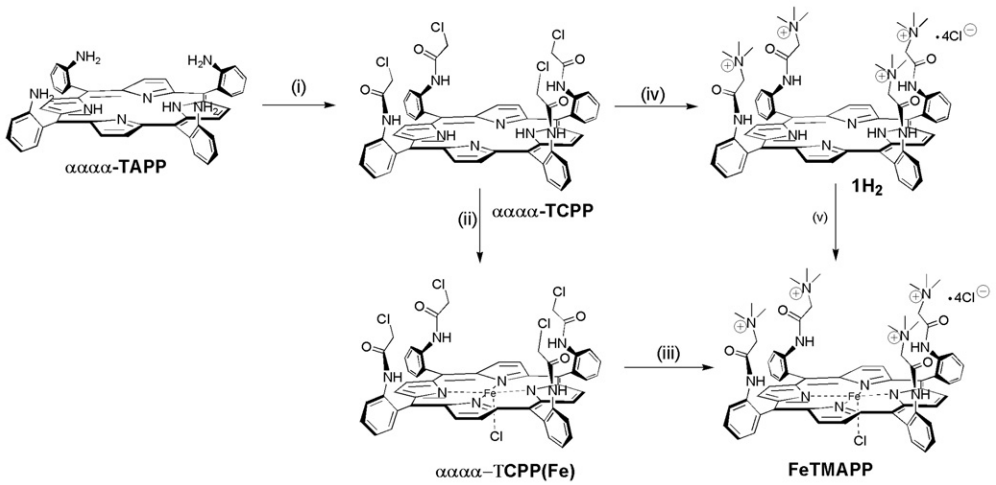

Scheme 1. Synthesis of cationic picket-fence porphyrin (FeTMAPP). (i) Chloroacetyl chloride in CH_2Cl_2, stirring at RT for 3 h; (ii) $FeBr_2$ in THF/benzene, reflux in N_2 for 2 h; (iii) and (iv) trimethylamine in ethyl alcohol in N_2 at RT, overnight.

was then washed with distilled water to remove nonadsorbed FeTMAPP. The obtained MWNTs-FeTMAPP nanocomposites could be dispersed in 1 mL doubly distilled water again by sonication, to obtain a stable nanocomposites suspension (photo c, Fig. 1).

2.4. Preparation of GNP/MWNTs-FeTMAPP nanocomposite self-assembled monolayer modified electrode

Gold disc electrodes (CH Instruments Inc., USA, 2.0 mm in diameter) were abraded with fine silicon carbide paper, successively polished with 0.3- and 0.05-μm alumina slurry, and sonicated in water and absolute ethanol. As shown in Fig. 1, the cysteamine self-assembled monolayer (Au/Cys) was firstly prepared by immersing the cleaned gold electrode in 0.1 M cysteamine at 4 °C overnight and washed with distilled water. This electrode was then immersed in GNP solution at 4 °C for 12 h to form a GNP self-assembled monolayer via the interaction between the exposed $-NH_2$ of cysteamine and GNP [24]. After washing with distilled water, the resulting GNP modified electrode was immersed in 1.5 mg mL^{-1} MWNTs-FeTMAPP nanocomposite suspension overnight to form MWNTs-FeTMAPP self-assembled monolayer through electrostatic interaction between the negatively charged GNP and the positively charged MWNTs-FeTMAPP nanocomposite. The resulting GNP/MWNTs-FeTMAPP modified electrode was washed with doubly distilled water and stored at 4 °C in air. As control, a GNP/FeTMAPP modified gold electrode was prepared with a similar procedure.

3. Results and discussion

3.1. Characteristics of MWNTs-FeTMAPP

As shown in Fig. 1, it was difficult to disperse the pristine MWNTs in water because of its hydrophobic surface

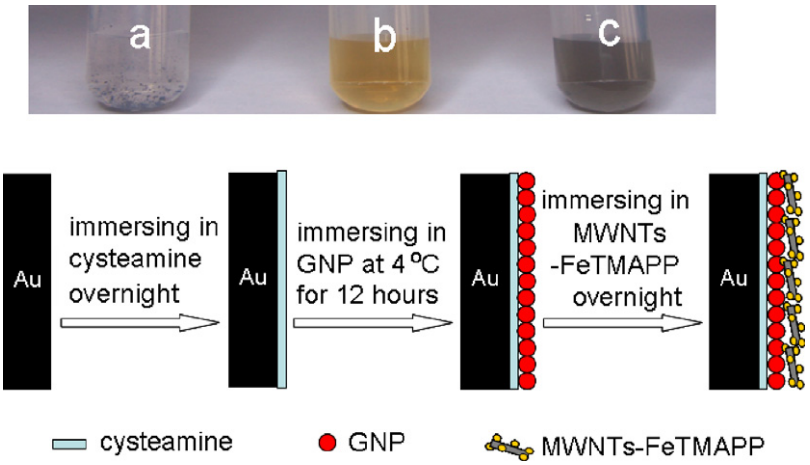

Fig. 1. Photos of (a) pristine MWNTs, (b) FeTMAPP solution and (c) MWNTs-FeTMAPP dispersion and fabrication process of self-assembled GNP/MWNTs-FeTMAPP monolayer.

(photo a, Fig. 1). FeTMAPP was soluble in water (photo b, Fig. 1), and its adsorption on MWNTs through the strong π–π stocking force produced MWNTs-FeTMAPP nanocomposites, which greatly improved the dispersion of MWNTs in water due to the hydrophilicity of the adsorbed FeTMAPP molecules (photo c, Fig. 1). The suspension of the nanocomposites was stable for at least one month, which highly facilitated the application of MWNTs in development of biosensors.

The UV–vis absorption spectra of FeTMAPP, MWNTs-FeTMAPP, and oxidized MWNTs are shown in Fig. 2. FeTMAPP solution exhibited a typical porphyrin visible spectrum (curve a, Fig. 2), with Soret band at 414 nm and several weaker absorptions (Q bands) at longer wavelengths (500–700 nm). MWNTs-FeTMAPP dispersion (curve b, Fig. 2) showed similar UV–visible spectrum with FeTMAPP solution, besides the faintness of Q bands, while the oxidized MWNTs dispersion did not show obvious adsorption (curve c, Fig. 2). The Soret band of MWNTs-FeTMAPP showed a decrease of intensity with a red shift from 414 nm to 421 nm, indicating the formation of J-typed aggregate nucleated on MWNTs [21].

3.2. Assembly and electrochemical characterization of GNP/MWNTs-FeTMAPP

FeTMAPP is positively charged in aqueous solution at pH 7.0, which makes it suitable to construct self-assembly monolayer through electrostatic interaction. Fig. 3A shows the cyclic voltammograms of the bare and modified electrodes in 0.1 M KCl containing 1.0 mM $[Fe(CN)_6]^{3-}$. Due to the electrode reaction of $[Fe(CN)_6]^{3-/4-}$ redox couple, the bare gold electrode exhibited a pair of well-defined redox peaks (curve a). Upon formation of GNP monolayer, the redox peak currents slightly increased and the peak-to-peak separation decreased (curve b), indicating the presence of GNP could prompt the electron transfer and improve the reversibility of electrode reaction [25]. At MWNTs-FeTMAPP modified electrode the redox peak currents greatly increased (curve c), which was attributed to the larger apparent surface of electrode due to the presence of nanocomposite.

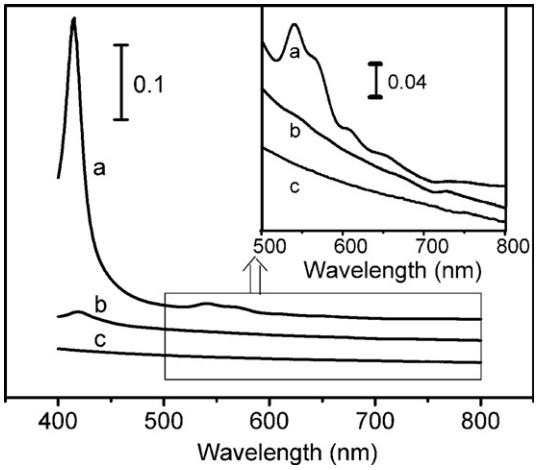

Fig. 2. UV spectra of (a) 0.34 mg mL^{-1} FeTMAPP solution, (b) 0.38 mg mL^{-1} MWNTs-FeTMAPP nanocomposites and (c) 0.38 mg mL^{-1} oxidized MWNTs suspensions.

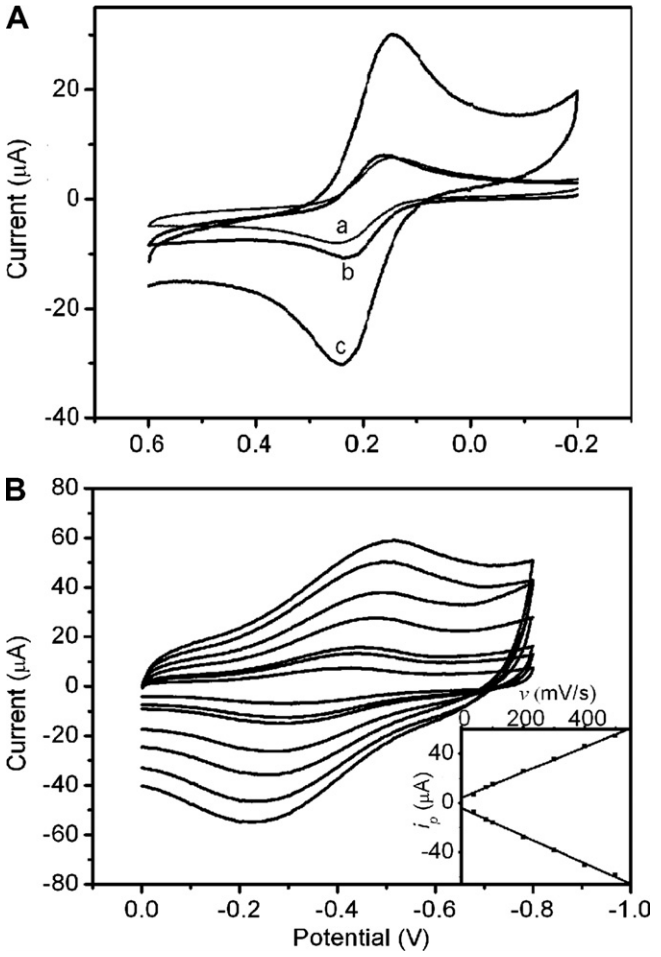

Fig. 3. Cyclic voltammograms of (A) bare (a), GNP (b) and GNP/MWNTs-FeTMAPP (c) modified electrodes in 0.1 M KCl containing 1.0 mM $[Fe(CN)_6]^{3-}$ at 100 mV s^{-1} and (B) GNP/MWNTs-FeTMAPP modified electrode in nitrogen-saturated PBS at 40, 80, 100, 200, 300, 400 and 500 mV s^{-1} (from inner to outer). Inset: plots of oxidation and reduction peak currents *vs.* *v*.

The GNP/MWNTs-FeTMAPP modified electrode showed a pair of redox peaks at −0.326 V and −0.400 V in nitrogen-saturated PBS at 40 mV s^{-1} (Fig. 3B), which were attributed to the electrode reaction of $Fe^{(III)}$TMAPP/$Fe^{(II)}$TMAPP redox couple. Both the oxidation and reduction peak currents were proportional to the scan rate (inset, Fig. 3B), indicating a surface controlled electrode process.

The amount of FeTMAPP adsorbed on electrode surface could be evaluated from the integration of the anodic or cathodic current peak area of $Fe^{(III)}$TMAPP/$Fe^{(II)}$TMAPP redox couple. The value was estimated to be 5.15×10^{-9} mol cm^{-2}, which was larger than those of 3.8×10^{-11} mol cm^{-2} for cobalt tetramethoxyphenyl

porphyrin [4] and 2.7×10^{-9} mol cm^{-2} for hemin/MWNTs [26] modified electrode. The coverage value was much larger than the monolayer coverage of FeTMAPP molecules. This was obviously due to a mass of FeTMAPP molecules in the nanocomposite.

The redox potential of FeTMAPP in the monolayer showed strong dependence on the pH value of the external solution. With an increasing pH the formal potential, midpoint of reduction and oxidation potentials, shifted negatively, exhibiting a linear relationship with a slope of -52.4 mV pH^{-1} over a pH range from 3.5 to 8.0. This value was very close to -57.6 mV pH^{-1}, the theoretical value at 18 °C, indicating one proton participated in the one-electron redox process. The electrode reaction could be described as follows:

$$\text{MWNTs-Fe}^{(\text{III})}\text{TMAPP}(\text{H}_2\text{O})(\text{OH}) + \text{H}^+ + \text{e}^- \rightarrow \text{MWNTs-Fe}^{(\text{II})}\text{TMAPP}(\text{H}_2\text{O})_2$$

3.3. Electrocatalytic reduction of dissolved oxygen on GNP/MWNTs-FeTMAPP modified electrode

The reduction of dissolved oxygen at bare gold electrode occurred at -0.2 V with a reduction peak potential of -0.5 V (curve b, Fig. 4A). After the self-assembly of GNP, the electrochemical behavior changed slightly in PBS saturated with nitrogen, but the starting potential for the reduction of dissolved oxygen shifted to -0.14 V, and the reduction peak current increased (curve b, Fig. 4B). The presence of GNP prompted the electron transfer of dissolved oxygen at electrode surface and catalyzed its reduction [27].

The GNP/FeTMAPP modified electrode exhibited better catalysis to the reduction of dissolved oxygen than GNP modified electrode (Fig. 4C), leading to a lower overpotential with a starting reduction potential of -0.08 V and a reduction peak at -0.38 V. This came from the presence of FeTMAPP, which meant that FeTMAPP could electrocatalyzed the reduction of dissolved oxygen, thus the reduction and oxidation peak currents of FeTMAPP increased and decreased, respectively. The relatively lower reduction current of dissolved oxygen than that at GNP modified electrode might be due to the decreasing apparent area upon adsorption of FeTMAPP on GNP.

At the GNP/MWNTs-FeTMAPP modified electrode the electrocatalysis toward the reduction of dissolved oxygen was further enhanced. As shown in Fig. 4D, the starting potential for the reduction of dissolved oxygen shifted to -0.0 V and the reduction peak occurred at -0.25 V. The reduction peak current also greatly increased. Compared with the electrocatalysis of MWNTs due to the metal impurities in CNT sample [28,29], the presence of MWNTs could prompt the electron transfer and increase the amount of FeTMAPP on electrode surface, exhibiting a synergy in electrocatalysis. FeTMAPP acted as electron transfer mediator to accelerate the reduction of dissolved oxygen, and MWNTs increased electron transfer rate, prompting the process of FeTMAPP mediated oxygen reduction.

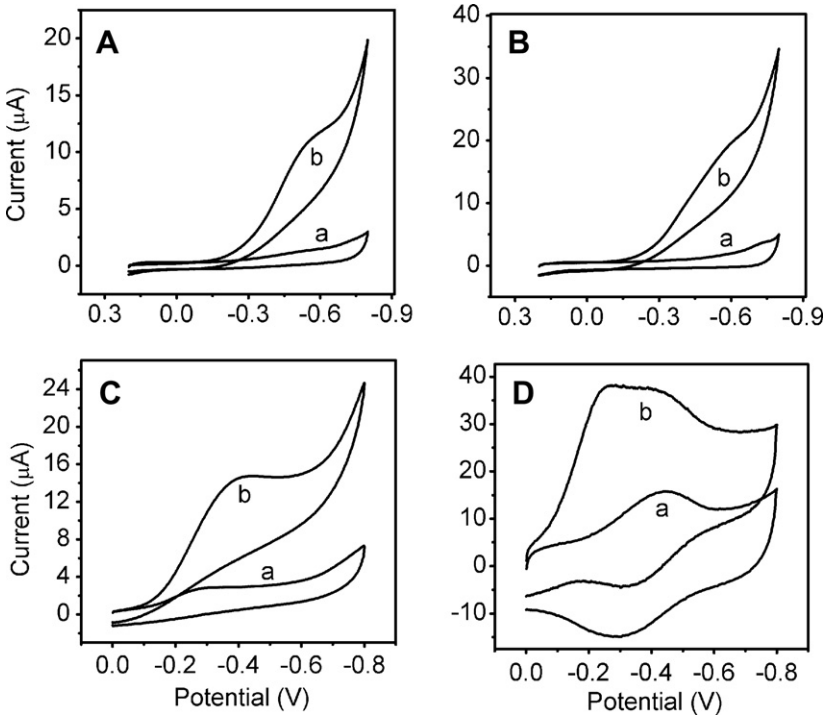

Fig. 4. Cyclic voltammograms of (A) bare electrode, (B) GNP, (C) GNP/FeTMAPP and (D) GNP/MWNTs-FeTMAPP modified electrodes in (a) nitrogen-saturated PBS and (b) oxygen-saturated PBS. Scan rate: 100 mV s^{-1}.

3.4. Performance of GNP/MWNTs-FeTMAPP self-assembled monolayer modified electrode as amperometric dissolved oxygen biosensor

Amperometric measurements were performed in a stirred PBS at an applied potential of −0.25 V. Fig. 5 shows the typical current–time responses of GNP/MWNTs-FeTMAPP self-assembled monolayer modified electrode to successive additions of oxygen saturated PBS. A sharp increase of current was observed after each addition of oxygen, and the response reached 98% of the steady state value within 4 s, showing a very fast response. With the saturated concentration of 2.6×10^{-4} mol L^{-1} for dissolved oxygen in water [30], its linear calibration range at the modified electrode was from 0.52 to 180 μM ($R = 0.997$, $n = 21$) (inset, Fig. 5), wider than 15–45 μM of the biosensor based on VB_{12}[31], and 0.06–4 μM at 2,2'-azino-bis(3-ethylbenzothiazoline-6-sulfonic acid) and laccase modified electrode [32]. The sensitivity of the proposed modified electrode was about 59.4 μA mM^{-1} with the detection limit of 0.38 μM at a signal-to-noise ratio of three. The effects of common interfering species on the biosensor response were examined. The injection of the same concentration of ascorbic acid (AA) or uric acid (UA) did not interfere with the amperometric response of dissolved oxygen. Besides, the detection potential of −0.25 V, more positive than those at other amperometric oxygen biosensors, avoided the interference of electrochemically reducible compounds.

The reproducibility and storage stability of the GNP/MWNTs-FeTMAPP self-assembled monolayer modified electrode were examined. The relative standard deviation (RSD) for the detection of dissolved oxygen with three electrodes prepared independently under the same conditions was 2.1%. When the biosensor was stored in dry at 4 °C and measured everyday, it retained about 84% of its original sensitivity after 2 weeks.

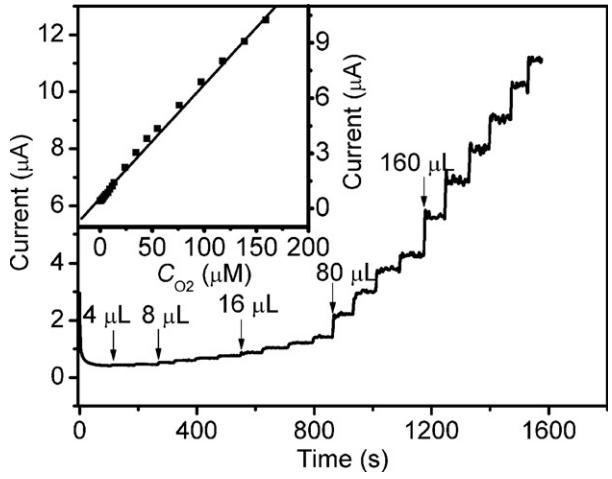

Fig. 5. Amperometric responses of GNP/MWNTs-FeTMAPP modified electrode to successive additions of oxygen-saturated PBS into a stirred nitrogen-saturated PBS at −0.25 V. Inset: calibration curve.

4. Conclusions

A simple method is proposed to prepare a kind of nanocomposites of MWNTs and FeTMAPP with good dispersion in water. The nanocomposites can be conveniently used to construct a GNP/MWNTs-FeTMAPP self-assembled monolayer modified electrode and develop a sensitive amperometric oxygen biosensor. The synergy of MWNTs and FeTMAPP enhances the electrocatalytic action of FeTMAPP to the reduction of dissolved oxygen. The sensitive detection of dissolved oxygen would provide a potential application of the nanocomposite and monolayer for preparing the biosensors of oxidase substrates. The supramolecular complex of charged metalloporphyrin and MWNTs provides a new insight to mimic the catalytic processes of the heme-containing enzymes.

Acknowledgements

This work was supported by the National Science Fund for Distinguished Young Scholars (20325518) and Creative Research Groups (20521503), the Key Program (20535010) and Special Program (20745003) from the National Natural Science Foundation of China, and the Science Foundation of Jiangsu (BK 2007570).

References

[1] R.T. Bailey, F.R. Cruickshank, G. Deans, R.N. Gillanders, M.C. Tedford, Anal. Chim. Acta 487 (2003) 101.
[2] T.M. Freeman, W.R. Seitz, Anal. Chem. 53 (1981) 98.
[3] P. Westbroek, E. Temmerman, Anal. Chim. Acta 437 (2001) 95.
[4] H.S. Liu, L. Zhang, J.J. Zhang, D. Ghosh, J. Jung, B.W. Downing, E. Whittemore, J. Power Sources 161 (2006) 743.
[5] Z. Ogumi, K. Matsuoka, S. Chiba, M. Matsuoka, Y. Iriyama, T. Abe, M. Inaba, Electrochemistry 70 (2002) 980.
[6] H.T. Zhao, H.X. Ju, Anal. Biochem. 350 (2006) 138.
[7] Y. Liu, S. Wu, H.X. Ju, L. Xu, Electroanalysis 19 (2007) 986.
[8] J.H. Ray, Y. Chan, S. Oliver, T. Kuwana, Inorg. Chem. 24 (1985) 3777.
[9] C. Shi, F.C. Anson, J. Am. Chem. Soc. 113 (1991) 9546.
[10] Y. Li, Z. Gan, N. Wang, X. He, Y. Li, S. Wang, H. Liu, Y. Araki, O. Ito, D. Zhu, Tetrahedron 62 (2006) 4285.
[11] J.Y. Qu, Y. Shen, X.H. Qu, S.J. Dong, Electroanalysis 16 (2004) 1444.
[12] Y.W. Chi, J.Y. Chen, M. Miyake, Electrochem. Commun. 7 (2005) 1205.
[13] B. Duong, R. Arechabaleta, N.J. Tao, J. Electroanal. Chem. 447 (1998) 63.
[14] Y.L. Zhang, C.X. Zhang, H.X. Shen, Electroanalysis 13 (2001) 1431.
[15] W.J.R. Santos, A.L. Sousa, R.C.S. Luz, F.S. Damos, L.T. Kubota, A.A. Tanaka, S.M.C.N. Tanaka, Talanta 70 (2006) 588.
[16] N. Zheng, Y. Zeng, P.G. Osbome, Y. Li, W. Chang, Z. Wang, J. Appl. Electrochem. 32 (2002) 129.
[17] C.M. Cordas, A.S. Viana, S. Leupold, F.P. Montforts, L.M. Abrantes, Electrochem. Commun. 5 (2003) 36.
[18] D.M. Guldi, G.M.A. Rahman, F. Zerbetto, M. Prato, Accounts Chem. Res. 38 (2005) 871.
[19] D. Baskaran, J.W. Mays, X.P. Zhang, M.S. Bratcher, J. Am. Chem. Soc. 127 (2005) 6916.

[20] D.M. Guldi, G.M. Rahman, J. Ramey, M. Marcaccio, D. Paolucci, F. Paolucci, S.H. Qin, W.T. Ford, D. Balbinot, N. Jux, N. Tagmatarchis, M. Prato, Chem. Commun. (2004) 2034.
[21] J.Y. Chen, C.P. Collier, J. Phys. Chem. B 109 (2005) 7605.
[22] J.P. Collman, Y. Yan, T. Eberspacher, X. Xie, E.I. Solomon, Inorg. Chem. 44 (2005) 9628.
[23] Y. Xiao, H.X. Ju, H.Y. Chen, Anal. Chim. Acta 391 (1999) 73.
[24] Y. Xiao, H.X. Ju, H.Y. Chen, Anal. Biochem. 278 (2000) 22.
[25] W.L. Cheng, S.J. Dong, E.K. Wang, Langmuir 18 (2002) 9947.
[26] J.S. Ye, Y. Wei, W.D. Zhang, H.F. Cui, L.M. Gan, G.Q. Xu, F.S. Sheu, J. Electroanal. Chem. 562 (2004) 241.
[27] M.S.E. Deab, T. Ohsaka, Electrochem. Commun. 4 (2002) 288.
[28] C.E. Banks, A. Crossley, C. Salter, S.J. Wilkins, R.G. Compton, Angew. Chem. Int. Ed. 45 (2006) 2533.
[29] X. Dai, G.G. Wildgoose, R.G. Compton, Analyst 131 (2006) 901.
[30] H.X. Ju, C.Z. Shen, Electroanalysis 13 (2001) 8.
[31] M.S. Lin, H.J. Leu, C.H. Lai, Anal. Chim. Acta 561 (2006) 164.
[32] C. Mousty, L. Vieille, S. Cosnier, Biosens. Bioelectron. 22 (2007) 1733.